Vibration Compensation in Optical Tracking Systems

Enrique Barbieri,* Ümit Özgüner,† and Stephen Yurkovich‡
Ohio State University, Columbus, Ohio

Modeling and control of multiple-mirror/flexible-slewing structures are considered. Primary applications for such systems include line-of-sight pointing systems on large flexible structures, space telerobotic systems, and space telescope systems. Analysis can be accomplished in a four-stage process: 1) relegation of control tasks; 2) flexible structure modeling and the slewing control problem; 3) vibration compensation using mirror actuators; and 4) active vibration damping with additional (structural) actuation. In the present paper, the first and third stages of the process are addressed. Relegation is achieved under the assumption that the optical ray hits the center of the following mirror along the ray path. Vibration compensation is then cast into the framework of a decentralized servocompensator problem. A recently developed optimal solution approach is utilized. A particular system is examined in detail, and control simulations are included to illustrate the results.

I. Introduction

OVER the last two decades, the increasing demands placed on lightweight design and construction of large space structures have led to a significant need for tight control requirements, especially for objectives such as pointing and rapid reorientation. Moreover, these control objectives must be achieved to facilitate the various functions of large satellites, spacecraft, and space telescopes, which include surveillance, defense, space exploration, astronomy, and general communications. Several programs have been oriented toward NASA's Space Station, where it is projected that nearly half of the experiments involved will require some form of pointing control systems for various line-of-sight (LOS) requirements.[1] That is, simultaneous control of attitude and LOS tasks (such as communication beam orientation) plays a major role in controller design.[2] On the topic of optical systems and mirror control, NASA's large Space Telescope,[3] requiring high-precision imaging through wavefront and pointing control, serves as a prime example. Active optics for compensation of wavefront distortion[4-6] and, to a lesser degree, optical ray pointing,[7] present challenging problems from a control design perspective on current and future space telescope systems. Other experimental setups arising mainly from the Active Control of Space Structures program that consist of a flexible supporting structure/mirror system include Draper model 2,[8] the Joint Optics Structures Experiment,[9,10] and the Rapid Retargeting and Precision Pointing (R2P2) experiment.[11] The primary goal in all of these efforts is to meet stringent LOS and jitter control requirements to accommodate disturbances of realistic size and bandwidth, where typical control functions may include target acquisition and tracking, pointing and rapid retargeting and so on. To that end, several types of control ideas are being studied, such as the design and experimental validation of on-off thrusters that minimize structural vibrations, hub control, proof-mass actuation on the structure, and distributed control and sensing.[12] Minimum-time reorientation maneuvers have been considered recently as a direct application of the current on-off control technology.[13,14] A positivity design approach has been applied to the Draper model 2,[15] a robustness optimization method has been applied successfully to a reduced-order model of the R2P2 experiment,[11] and optics control issues were discussed and evaluated for the Large Optics Demonstration Experiment (LODE) and LODE Advanced Mirror Program.[10] These works have also stimulated the study of single-plane and segmented-mirror control systems, such as in Ref. 16, for robust control in the presence of disturbances acting on the system from control forces, power systems, or other external forces.

In this paper, we propose analysis and control design for optical tracking systems, in general, in a four stage process: 1) Relegation of control tasks; 2) Flexible structure modeling and the slewing control problem; 3) Vibration compensation using mirror actuators; and 4) Active vibration damping with additional (structural) actuation. Clearly, it is not possible to consider the complete problem and the ramifications of selecting a particular modeling/control technique in one single paper. Therefore, only the first and third stages of the preceding process are addressed here. Relegation is one of the most critical issues in controller design for such systems, and involves decisions on how to optimally utilize the various effectors (mirror/actuator systems) with different dynamic range capabilities and bandwidth characteristics; methods of decentralization[17-19] thus play an important role. Similar issues exist for the use of sensed information regarding disturbance vibrations in the design of active damping in structural control. A strategy of major importance toward these ends that is investigated is the merging of centralized and decentralized control schemes as dictated by the physical system and modeling thereof. For example, assuming that individual mirror systems have position and rate sensing locally available only to that system, it is reasonable to design local control in a decentralized setting relegated precisely for tilt and rotation. On the other hand, for example, slewing control is better cast in a centralized setting. In the present study, we shall assume that the relevant relegation problem is that of *set-point relegation* for the mirror actuators.

The primary contribution of this work involves investigation of issues related to the modeling and control of flexible structures on which are mounted movable mirrors for optical ray-tracing systems *after slew and reorientation maneuvers*. That is, we assume that the slewing maneuver has been accomplished; the problem is now that of *mirror control* for ray pointing to accommodate the flexible disturbance introduced by the vibrating structure. In the next section, the mirror actuator control is cast into the framework of a decentralized servocompensator problem. Section III contains the development for a specific optical tracking system. Section

Received Oct. 30, 1987; revision received April 18, 1988.

*Ph.D. Candidate, Department of Electrical Engineering; currently with the Department of Electrical Engineering, Tulane University, New Orleans, LA. Member AIAA.

†Professor, Department of Electrical Engineering. Member AIAA.

‡Assistant Professor, Department of Electrical Engineering.

IV describes the design of a reduced-order optimal servocompensator. Control simulations illustrating the design are included.

II. Problem Formulation

We consider a general optical tracking system consisting of a large flexible supporting structure on which a number of rigid mirrors are mounted that can be independently controlled for precision ray pointing. The (decentralized) mirror control problem is then the design of a local servocompensator, which will regulate the local pointing error against unwanted disturbances.

We will assume that the coupling between actuator dynamics and the associated rigid-body dynamics may be modeled as a linear, time-invariant (LTI) system for which a controller, or decentralized controllers, are to be designed. Furthermore, the vibrations induced by the flexible structure are modeled as additive disturbances to the mirror positions. These effects may be modeled a priori but not measured on-line. Consider, then, the general LTI system consisting of v control agents described by

$$\dot{x} = Ax + \sum_{i=1}^{v} B_i u_1 + E\delta \tag{1}$$

$$y_1 = C_i x + D_i u_i + F_i \delta, \qquad e_i = y_i - y_i^r, \quad i = 1,...,v \tag{2}$$

where $x \in \mathbf{R}^n$ is the state, $u_i \in \mathbf{R}^{m_i}$ and $y_i \in \mathbf{R}^{r_i}$ are the input and the output for the ith control agent ($i = 1,...,v$), respectively, and $\delta \in \mathbf{R}^l$ is an unmeasurable disturbance satisfying

$$\ddot{q} = \mathbf{A}_1 q, \qquad \delta = T_1 q \tag{3}$$

which is a model of the flexible structure that retains l modes, and could be obtained by using finite-element techniques or from finite modal expansions of the appropriate equations of motion.[20–22] The ith error $e_i \in \mathbf{R}^{r_i}$ is the difference between y_i and a specified reference input

$$y_i^r = G_i \sigma + H_i q, \quad i = 1,...,v \tag{4}$$

where $\sigma \in \mathbf{R}^p$ satisfies

$$\dot{\sigma} = \mathbf{A}_2 \sigma \tag{5}$$

Note that Eq. (4) implies that the reference signal also may contain frequencies of the vibrating structure. Furthermore, it is assumed that the output

$$y_i^m = C_i^m x + D_i^m u_i + F_i^m \delta$$

where $y_i^m \in \mathbf{R}^{r_i m}$ is available for measurement by the ith control agent ($i = 1,...,v$). All matrices involved are constant and appropriately dimensioned.

The optimal decentralized controllers for system (1) are of the form

$$u_i = K_i^1 \tilde{y}_i + K_i^2 \eta_i, \quad i = 1,...,v \tag{6}$$

where $\tilde{y}_i \triangleq y_i^m - D_i^m u_i$, and η_i is the output of the ith local optimal servocompensator given by

$$\dot{\xi}_i = A_{s_i} \xi_i + B_{s_i} e_i, \qquad \eta_i = C_{s_i} \xi_i$$

where the cost criterion chosen to be minimized and the definition of the compensator parameters are outlined in Appendix A. When such a controller exists, the ith error $e_i, i = 1,...,v$, is asymptotically driven to zero for all disturbances [Eq. (2)] and reference inputs [Eq. (3)] and the overall system is stable. A block diagram of the closed-loop system illustrating one local control loop is given in Fig. 1.

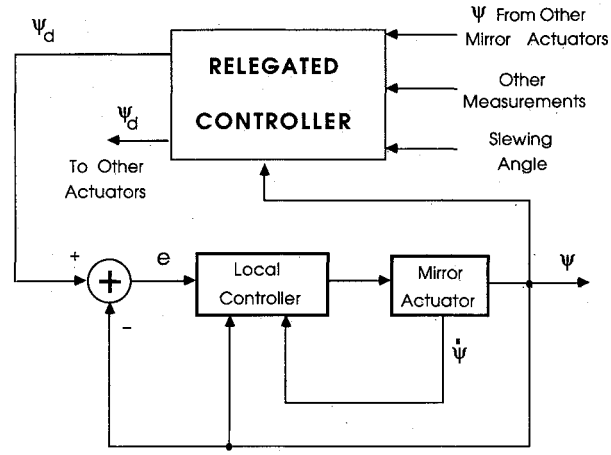

Fig. 1 Closed-loop system.

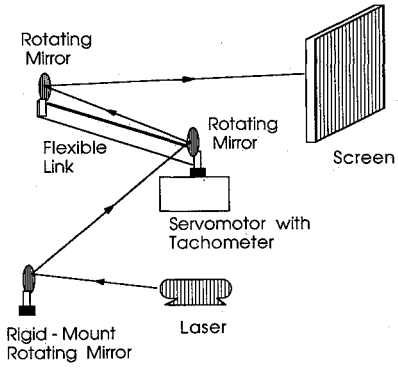

Fig. 2 Example mirror structure.

III. Optical Tracking System Example

Consider the planar multiple-mirror/flexible/slewing beam structure shown in Fig. 2. A complete model of the system has been developed,[23] which features hub slewing and structural actuation capabilities. In Appendix B, a detailed optical analysis is presented, which leads to a set of nonlinear, algebraic ray-path equations needed for controller design.

This configuration was chosen because it results in a simple mathematical formulation but yet poses challenging difficulties with regard to modeling and control. The first, stationary mirror (rigid mount) is added to the model since, *in an envisioned laboratory setup*, it would allow for easy manipulation of the ray origin while maintaining a stationary light source. The servomotor is used to slew the flexible beam; in future work, it will be incorporated into the design as part of time-optimal slewing control experiments. Although simplistic in design relative to large-scale space-based systems, this example is generic in nature to a point that it offers problems similar in spirit to those encountered in most projected large space structure applications for LOS regulation in optical tracking systems.

In this specific example, the interaction between the mirror motors and the beam is neglected so that the system model turns out to be uncoupled, as it only involves the three mirror actuator dynamics. Moreover, if an attempt had been made to do active structural damping simultaneously, the system dynamics would be coupled, which also involves structural parameters. Assume then that the mirror motors are identical and described by the following simplified state equations:

$$\dot{x}_i = A_m x_i + B_m u_i + E_i \delta$$

$$\theta_i = C_m x_i + F_i \delta, \qquad i = 1,2,3$$

where $x_i = [\psi_i \; \dot{\psi}_i]^T$, $i = 1,2,3$, and the mirror angles ψ_i,

$i = 1,2,3$, are defined in Appendix B. There are now three problems to be investigated: 1) modeling of the flexure effects, 2) specification of the individual set points for the mirror angles, and 3) design of the compensator.

Modeling of the Flexure Effects

The most widely accepted means for obtaining a finite-dimensional state-space representation for flexible structures is the well-known finite-element method. However, in the case of a simple structure, such as the slewing beam, the equations of motion can be solved analytically and an adequate model can be derived. A recent development[22] of a laboratory setup of an aluminum slewing beam will be used in this paper. The l-dimensional model in *modal* coordinates can be written as

$$\ddot{q} + \Omega^2 q = B\tau_b$$

where $\Omega \in \mathbf{R}^{l \times l}$ is a diagonal matrix of beam structural modes, $\tau_b(t)$ is the applied torque at the hub of the beam, and $q = [\psi_4\ \mathbf{r}]^T$, where $\psi_4(t)$ is the slewing angle and $\mathbf{r}(t)$ is a vector of modal coordinates. In this formulation, it has been assumed that the beam is uniform and homogeneous, and that only transverse and bending motions are of interest.

The vector of *physical* coordinates is composed of the local beam's displacements and their spatial derivatives (bending angles) at a finite number of nodes. This vector is the same as the disturbance vector defined earlier, and can be constructed by the relation

$$\delta = T_1 q$$

where T_1 is an orthogonal similarity transformation (modal matrix).

Specification of Mirror Set Points

As a control objective in controller design for this example system, we define the constant set-point problem as follows: given a desired y_d on the screen, solve the ray-path equations (see Appendix B) for the required angles ψ_1, ψ_2, ψ_3, and ψ_4. This is a difficult inverse kinematics problem, which, in general, has many solutions. One way to reduce the size of the solution space considerably is to force the ray to follow a *nominal trajectory*, which is chosen based on the particular geometry of the problem. In this manner, a local tracking problem can be defined for each mirror.

Cast in this ray-tracing formulation, we propose a control strategy based on the principle of maintaining the ray on the *center* of each mirror throughout the optical path; i.e., for this particular structure, the nominal trajectory is defined to be the line joining the centers of the primary, hub, and secondary mirrors, in that order. The relegation of set points to mirror actuators is, therefore, done by assuming that rays are to hit the center of the next mirror along the ray path. With this additional constraint and given the desired set point on the screen y_d and the slewing angle ψ_4, the required mirror settings are found to be

$$\psi_1 = \tfrac{1}{2}\arctan[\bar{y}_2/(\bar{x}_2 - \bar{x}_1)] \tag{7}$$

$$\psi_2 = \psi_1 - \tfrac{1}{2}\psi_4 \tag{8}$$

$$\psi_3 = \tfrac{1}{2}(\sigma_a + \psi_4) \tag{9}$$

where the angle σ_a is given by

$$\sigma_a = \arctan\left[\frac{y_d - \bar{y}_3}{x_S - \bar{x}_3}\right] \tag{10}$$

and the coordinate $(\bar{x}_3,\bar{y}_3)$ of the center of the tip mirror is simply

$$\bar{x}_3 = \bar{x}_2 - L\cos(\psi_4), \qquad \bar{y}_3 = \bar{y}_2 + L\sin(\psi_4)$$

where $(\bar{x}_2,\bar{y}_2)$ is the coordinate of the center of the hub mirror, and L is the undeformed length of the beam.

Coupling of problems 1 and 2 is achieved by defining a "flexibility angle" $\beta(t)$ that is approximated by $\beta(t) \approx y_{\text{tip}}/L$, where y_{tip} is the local displacement of the tip of the beam. In this case, the effective (flexible) slewing angle is $\psi_4' = \psi_4 + \beta$.

Design of the Compensator

A reduced-order optimal servocompensator has been designed and applied to the preceding motor models. [This design was not carried through for mirror motor 1, since it only needs to be adjusted (once) to the constant value given by Eq. (7).] The mirror control law is given by

$$u_i(t) = -K_i^1 x_i - K_i^2 \eta_i(t), \qquad i = 2,3 \tag{11}$$

where $\eta_i(t)$ is the output of the ith servocompensator

$$\dot{\xi}_i = A_{s_i}\xi_i + B_{s_i} e 1, \qquad \eta_i = C_{s_i}\xi_i, \quad i = 2,3$$

K_i^1, K_i^2, $i = 2,3$, are constant gains, and the triples $(A_{s_i},B_{s_i},C_{s_i})$, $i = 2,3$, are specified next.

Following the approach outlined in Sec. II and Appendix A, we define the characteristic polynomial of the compensator for mirror motors 2 and 3 to be

$$a(s) = s^5 + a_4 s^4 + a_3 s^3 + a_2 s^2 + a_1 s + a_0$$

where

$$a_4 = 2(\xi_i\omega_1 + \zeta_2\omega_2)$$

$$a_3 = \omega_1^2 + \omega_2^2 + 4\zeta_1\zeta_2\omega_1\omega_2$$

$$a_2 = 2\zeta_1\omega_1\omega_2^2 + 2\zeta_2\omega_2\omega_1^2$$

$$a_1 = \omega_1^2\omega_2^2$$

$$a_0 = 0$$

so that the first two modes of the system and the constant reference signal are tracked. The control law is then given by Eq. (11), where the gains (K_i^1,K_i^2), $i = 2,3$, are obtained by solving an appropriate Ricatti equation (see Ref. 24 for details) and the triples $(A_{s_i},B_{s_i},C_{s_i})$, $i = 2,3$, are constructed as follows:

$$A_{s_i} = T\begin{bmatrix} 0 & 1 & 0 & 0 & 0 \\ 0 & 0 & 1 & 0 & 0 \\ 0 & 0 & 0 & 0 & 0 \\ 0 & 0 & 0 & 0 & 1 \\ -a_0 & -a_1 & -a_2 & -a_3 & -a_4 \end{bmatrix} T^{-1}$$

$$B_{s_i} = T\begin{bmatrix} 0 \\ 0 \\ 0 \\ 0 \\ 1 \end{bmatrix} \qquad C_{s_i} = \begin{bmatrix} a_1 & a_2 & a_3 & a_4 & 1 \\ a_2 & a_3 & a_4 & 1 & 0 \\ a_3 & a_4 & 1 & 0 & 0 \\ a_4 & 1 & 0 & 0 & 0 \\ 1 & 0 & 0 & 0 & 0 \end{bmatrix} T^{-1}$$

where T is an arbitrary nonsingular transformation (set to identity in the simulations).

IV. Simulation Results

In this section, we present control simulations of the example mirror structure for the constant set-point problem described earlier. Since our present study does not address slewing control, we generate a slewing angle profile by selecting the following hub torque control law:

$$\tau_b = -K_{an}\psi_4 - K_{ve}\dot{\psi}_4 + \psi_4^d$$

for constant gains K_{an}, K_{ve} and desired hub angle ψ_4^d. The

Table 1 Physical properties and modes of the flexible beam

Material	Aluminum
Length, m	1
Cross section, m^2	1.5875×10^{-4}
Height, m	0.1
Young's modulus, N/m^2	6.8944×10^{8}
Linear density, kg/m	0.4847
Moment of area, m^4	3.334×10^{-11}

Structural modes, Hz	Closed-loop poles
0.0	$-2.09\,E-3 \pm j0.753$
0.4417	$-8.35\,E-2 \pm j4.72$
1.0591	$-6.14\,E-1 \pm j13.74$
2.3042	$-6.77\,E00 \pm j12.29$
4.3555	$-0.24\,E00 \pm j27.29$
7.1405	$-8.75\,E-2 \pm j44.85$
10.638	$-4.05\,E-2 \pm j66.83$
14.841	$-2.18\,E-2 \pm j93.24$
19.747	$-1.30\,E-2 \pm j124.08$

Table 2 RMS errors using servocompensator control

No. of modes sensed	EP_2, μrad	EP_3, μrad	E_{hit}, mm
2	0.2263	0.1549	94.76
4	0.6889	0.4831	2.684

mirror motor parameters (A_m, B_m, C_m) are taken to be

$$A_m = \begin{bmatrix} 0 & 1 \\ 0 & -314.16 \end{bmatrix}, \qquad B_m = \begin{bmatrix} 0 \\ 1 \end{bmatrix}, \qquad C_m = [1\ 0]$$

and to simplify the simulations we set matrices E_i and F_i to zero.

The physical dimensions, material properties, and the first nine structural modes of the beam are presented in Table 1. In this table, we also list the corresponding closed-loop poles for the choice of gains $(K_{an};K_{ve}) = (1.1;0.1)$. Figure 3 illustrates a 20-s time history of the slewing angle profile and of the beam-tip position for the full-order model also regarded as the *truth* model. (Programs were run on a VAX 11/785 computer in double-precision FORTRAN code.) In order to simulate the performance of a noiseless band-limited sensor, the flexibility angle β is generated from reduced-order models retaining two and four modes, and is used to develop the reference signals ψ^d for each mirror motor. The sampling time is $T_s = 0.005\ s$.

Initially, the structure is at rest with $x_s = -0.1$ m, $(\bar{x}_1,\bar{y}_1) = (-3.00,0.00)$ m, $(\bar{x}_2,\bar{y}_2) = (-1.25,0.75)$ m, $y_{hit} = 2.9$ m, and $\psi_4 = 55$ deg. A 25-deg slew and three new set points at different times are requested: $y_d = 1.9$ m at the start of the slew; $y_d = 2.0$ m at $t = 8.0$ s; and $y_d = 1.8$ m at $t = 14.0$ s. Figure 4 shows the behavior of the hub and tip mirrors and the resulting y_{hit} on the screen. These plots illustrate typical results corresponding to the case when four modes are being sensed. The transient lasts only for about 0.2 s and, realistically speaking, the ray should be off during this "lock-on-target" period of time. Observe that these simulations point out that there exist a set of targets reachable by mirror control only without requiring any further slewing action.

Consider now the case of tracking only the constant set point $y_d = 1.9$. The following figure of merit is defined as

$$\text{rms(data)} = \sqrt{\frac{1}{N}\sum_{i=1}^{N} (\text{data}_i)^2}, \qquad 4.0 \leqslant t \leqslant 20.0$$

where N is the number of data points. The rms tracking errors

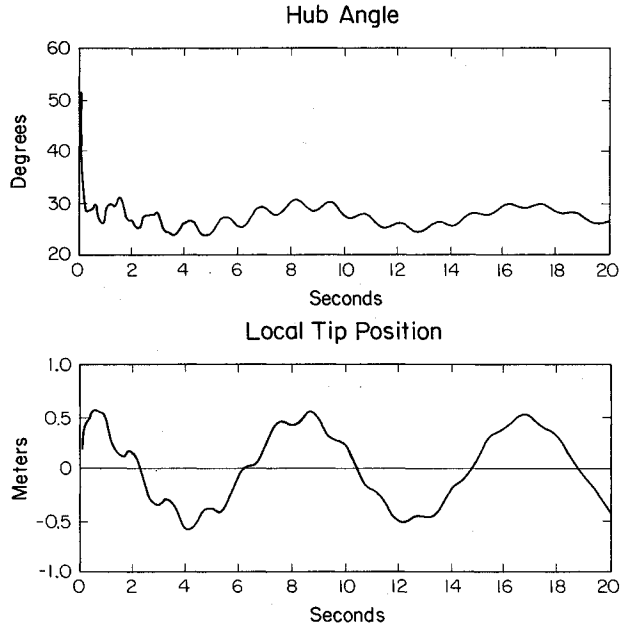

Fig. 3 Slewing angle and beam-tip position (full model).

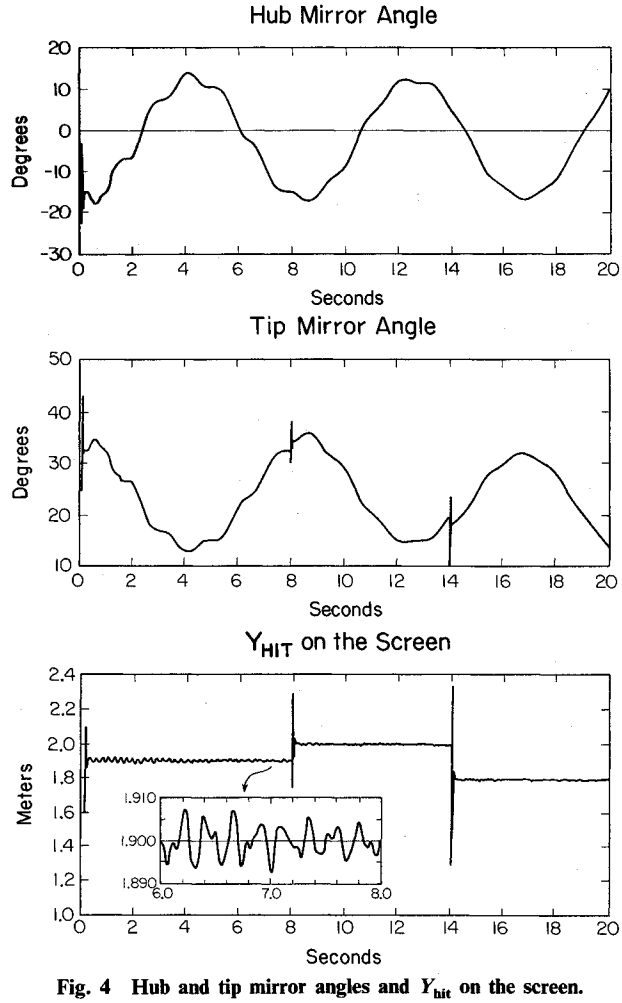

Fig. 4 Hub and tip mirror angles and Y_{hit} on the screen.

are defined as follows:

$$EP_2 \triangleq \psi_2^d - \psi_2, \qquad EP_3 \triangleq \psi_3^d - \psi_3, \qquad E_{hit} \triangleq y_{hit} - y_d$$

where y_{hit} is always computed based on the *truth* model. Table 2 lists our results for the controller designed in the previous section.

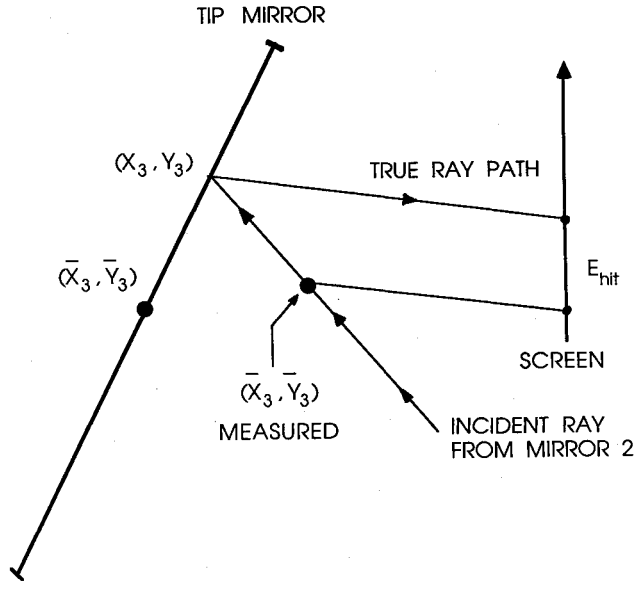

Fig. 5 E_{hit} caused by error in tip measurement.

We summarize our results by making the following observations:

1) The control design is robust in the sense that reasonable tracking performance is maintained when the control is applied to a higher-order truth model. Note that, when the servocompensator is required to track more than two modes, the result is simply a slight increase in EP_2 and EP_3 and a substantial decrease in E_{hit}.

2) We have also investigated the performance of a simple proportional control law,[25] and found comparable results as far as E_{hit} is concerned. However, a considerable improvement is observed in EP_2 and EP_3 when the servocompensator is used. This is to be expected because of the optimal nature of that design.

3) Our simulations illustrate that control relegation ideas may be applicable to decide whether to slew and by how much, and whether it is possible to reach a target by adjusting the mirrors only. Clearly, one choice of optimal policy is to slew the structure the least so that flexure disturbances are kept to a minimum.

4) Our study also indicates that a major design effort should be directed toward relegation of dynamic-range capabilities for the different mirror actuators. For example, it is clear that, if flexure effects are minimized, and depending on the target-tracking requirements, then, in the system described here, the tip mirror control may require a higher bandwidth than the hub mirror control. Further results on the issue of output set-point relegation may be found in Ref. 26.

5) We identify two sources of error in E_{hit}: 1) the mirror motor dynamics and 2) the lack of knowledge of the exact position of the tip of the beam. The effect of the motor dynamics may be reduced by employing very-high-bandwidth actuators. The contribution of the second error source is dominant however, and can be best demonstrated through a graphical illustration. Consider the case shown in Fig. 5, where we assume that the error caused by the motor dynamics is zero so that the ray goes through the point $(\bar{x}_3,\bar{y}_3)_{\text{measured}}$. It can be shown that, in this case, E_{hit} is proportional to $\Delta\beta$, where $\Delta\beta \ll 1$, and represents the sensor error due to bandwidth, resolution, or additive noise. Therefore, sensor error on the order of milliradians will *inevitably* result in E_{hit} being on the order of millimeters.

6) The previous discussion leads us to the idea of employing estimation schemes such as Kálmán filtering in an attempt to improve the accuracy of the measured tip information. Although some results along this line of research have been reported recently in a separate study,[27] we have not implemented such ideas in the designs of this paper. However, for the purpose of evaluating any positive effect of tip position prediction, we have investigated the rms tracking errors obtained when a proportional controller is based on the ideal "n-step-ahead predicted" information

$$\beta(t) = \beta(t + nT_s)$$

where T_s is the sampling time. The rms errors obtained with such a predictor are only slightly better; therefore, we are led to conclude that a real-time predicting scheme will increase the complexity of the controller further and may not improve the results appreciably.

7) We point out that the model used in this work does not include certain interactions, such as coupling between the hub mirror angle and slewing action and coupling between tip mirror actuation and structural deformations of the beam. Although we mentioned that a complete model already has been assembled, its use would necessarily involve slewing, active structural vibration damping, sensor dynamics, ray-path regulation, model-order reduction, and spillover issues. The overall control problem is obviously very complex. In this paper, we have initiated, identified, and put into focus some of the relevant problems in the design of controllers for optical tracking systems.

V. Conclusion

In this paper, we have considered issues arising in the modeling and control of optical ray-tracing mirror systems mounted on flexible structures. The problem has been cast in a decentralized framework, and the control strategies developed have been analyzed from a relegation viewpoint. Simulation studies have shown that fine line-of-sight control within bandwidth limitations of the actuation devices is possible, although very sophisticated sensing devices must be developed to match the expectation of high-accuracy pointing systems. The interconnection of several mirror systems and desired control actions is obviously a complex problem. For example, a recent study indicated potential problem areas regarding robustness (system sensitivity) due in part to cross-dynamic coupling. The decentralized/relegated control scheme described in this paper serves the purpose of illustrating a potential interconnection and control strategy, and can be used to specify a working model for controller analysis and design.

Appendix A

In this Appendix, we briefly outline the decentralized optimal servocompensator problem. The approach follows the one developed by İftar and Özgüner.[24] Let

$$\Lambda(s) = s^p + a_{p-1}s^{p-1} + \cdots + a_0 \tag{A1}$$

be the least common multiple of the characteristic polynomials of $\mathbf{A}_1$ and $\mathbf{A}_2$. Define the operator

$$S \triangleq \frac{d^p}{dt^p} + a_{p-1}\frac{d^{p-1}}{dt^{p-1}} + \cdots + a_1\frac{d}{dt} + a_0$$

where $a_0,a_1,\ldots,a_{p-1}$ are the scalars defined in Eq. (A1). Then let

$$\bar{x} \triangleq Sx, \qquad \bar{u}_i \triangleq Su_i, \qquad \epsilon \triangleq [\epsilon_1^T,\epsilon_2^T,\ldots,\epsilon_p^T]^T$$

where $(\cdot)^T$ denotes the transpose of $(\cdot)$,

$$\epsilon_1 \triangleq e^{(p-1)} + a_{p-1}e^{(p-2)} + \cdots + a_2 + a_1 e$$

$$\epsilon_2 \triangleq e^{(p-2)} + a_{p-1}e^{(p-3)} + \cdots + a_3 + a_2 e$$

$$\vdots$$

$$\epsilon_p \triangleq e$$

$(\cdot)^{(k)}$ denotes the kth time derivative of $(\cdot)$, $e \triangleq (e_1^T,...,e_v^T]^T$, and $z \triangleq [\bar{x}\ \varepsilon]^T$. Then we can write the augmented system

$$\dot{z} = \bar{A}z + \sum_{i=1}^{v} \bar{B}_i \bar{u}_i$$

where

$$\bar{A} = \begin{bmatrix} A & 0 & \cdots & 0 & 0 \\ C & 0 & \cdots & 0 & -a_0 I_r \\ 0 & I_r & & & \cdot \\ \cdot & \cdot & & & \cdot \\ \cdot & & \cdot & & \cdot \\ \cdot & & & & \cdot \\ 0 & & & I_r & -a_{p-1} I_r \end{bmatrix}, \qquad \bar{B}_i = \begin{bmatrix} B_i \\ D_i^* \\ 0 \\ \cdot \\ \cdot \\ \cdot \\ 0 \end{bmatrix}$$

$$D_i^* \triangleq [0_{m_i \times \Sigma_{j=1}^{i-1} r_j}, D_i^T, 0_{m_i \times \Sigma_{j=i+1}^{v} r_j}]^T$$

$$C \triangleq [C_1^T,...,C_v^T]^T, \qquad r \triangleq \sum_{i=1}^{v} r_i$$

and I_k denotes the $k \times k$ identity matrix.

Next, we define the following cost function to be minimized:

$$J = \int_0^\infty \left(z^T Q z + \sum_{i=1}^{v} \bar{u}_i^T R_i \bar{u}_i \right) dt \qquad \text{(A2)}$$

where $Q = Q^T \geqslant 0$, $R_i = R_i^T > 0$, $i = 1,...,v$.

The optimal control law is given by Eq. (6), where the decentralized servocompensator parameters are constructed in the following manner:

$$A_{s_i} = T \begin{bmatrix} 0 & I_{r_i} & & 0 \\ \vdots & & \ddots & \\ 0 & 0 & & I_{r_i} \\ -a_0 I_{r_i} & -a_1 I_{r_i} & \cdots & -a_{p-1} I_{r_i} \end{bmatrix} T^{-1}$$

$$B_{s_i} = T \begin{bmatrix} 0 \\ \vdots \\ 0 \\ I_{r_i} \end{bmatrix} \qquad C_{s_i} = \begin{bmatrix} a_1 I_{r_i} & a_2 I_{r_i} & \cdots & a_{p-1} I_{r_i} & I_{r_i} \\ a_2 I_{r_i} & a_3 I_{r_i} & \cdots & I_{r_i} & 0 \\ \vdots & & & 0 & \\ I_{r_i} & & & & \end{bmatrix} T^{-1}$$

T is a nonsingular transformation matrix, and the constant gain matrices K_i^1 and K_i^2 satisfy an appropriate Riccati equation (see Ref. 24 for details).

We can then state that, under certain controllability/observability and rank conditions, the controller described by Eq. (6) exhibits the following properties[24]:

1) Asymptotic regulation takes place for all disturbances and for all reference inputs, as described in Sec. II.

2) The overall system is stable.

3) The cost, given by Eq. (A2), is minimized.

4) If the disturbance δ and the reference input y_r are bounded, then the input u is bounded.

5) The controller is robust with respect to a class of system parameter perturbations.

Appendix B

In this Appendix, we outline a general methodology that can be used to obtain the ray-path equations in multiple-mirror/flexible-slewing structures. The approach developed here borrows the standard mathematical notation used to describe the direct kinematics of robotic manipulators.

In order to introduce the notation used throughout, consider two coordinate frames $\{A\}$ and $\{B\}$ as shown in Fig. B1, where

$\hat{(\cdot)}_A$ = unit vector in the $(\cdot)$ direction of coordinate frame A

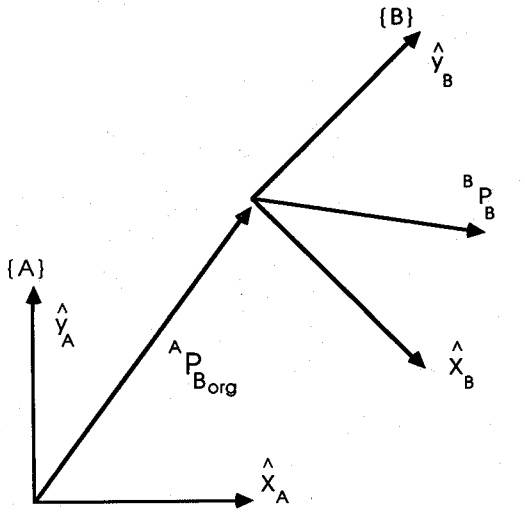

Fig. B1 Two-dimensional coordinate frames.

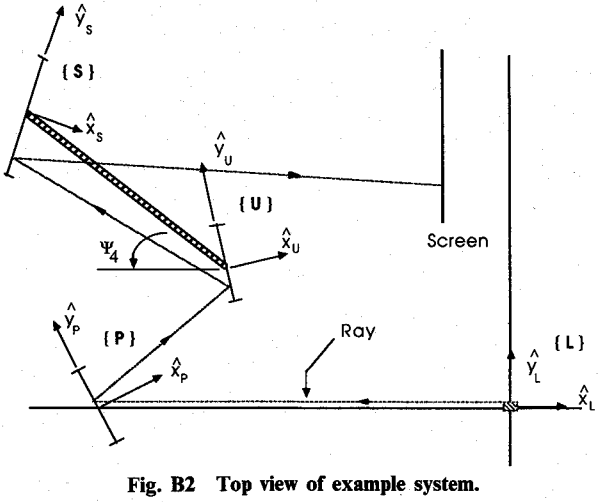

Fig. B2 Top view of example system.

${}^A P_B$ = any point in frame B referenced to frame A

${}^A P_{B_{org}}$ = vector connecting the origins of frames A and B

The vector ${}^B P_B$ in frame B is represented in frame A according to

$$\begin{bmatrix} {}^A P_B \\ 1 \end{bmatrix} = {}_B^A T \begin{bmatrix} {}^B P_B \\ 1 \end{bmatrix} \quad \text{or} \quad {}^A P_B = {}_B^A R\, {}^B P_B + {}^A P_{B_{org}}$$

where ${}_B^A T$ is the 3×3 homogeneous coordinate frame transformation matrix and ${}_B^A R$ is the 2×2 orthogonal rotation matrix given by, respectively,

$${}_B^A T \triangleq \begin{bmatrix} {}_B^A R & {}^A P_{B_{org}} \\ 0 & 1 \end{bmatrix}, \qquad {}_B^A R \triangleq \begin{bmatrix} \cos\theta_{BA} & \sin\theta_{BA} \\ -\sin\theta_{BA} & \cos\theta_{BA} \end{bmatrix}$$

where θ_{BA} is the angle between $\hat{x}_B$ and $\hat{x}_A$ and is positive when measured counterclockwise.

Consider the top view of the mirror structure as shown in Fig. B2. Define the homogeneous frame transformations

$${}_P^L T \triangleq \begin{bmatrix} {}_P^L R & {}^L P_{P_{org}} \\ 0 & 1 \end{bmatrix}; \qquad {}^L P_{P_{org}} \triangleq \begin{bmatrix} \bar{x}_1 \\ 0 \end{bmatrix}$$

$${}_U^L T \triangleq \begin{bmatrix} {}_U^L R & {}^L P_{U_{org}} \\ 0 & 1 \end{bmatrix}; \qquad {}^L P_{U_{org}} \triangleq \begin{bmatrix} \bar{x}_2 \\ \bar{y}_2 \end{bmatrix}$$

$${}_S^L T \triangleq \begin{bmatrix} {}_S^L R & {}^L P_{S_{org}} \\ 0 & 1 \end{bmatrix}; \qquad {}^L P_{S_{org}} \triangleq \begin{bmatrix} \bar{x}_3 \\ \bar{y}_3 \end{bmatrix} = \begin{bmatrix} \bar{x}_2 - L\cos\psi_4 \\ \bar{y}_2 + L\sin\psi_4 \end{bmatrix}$$

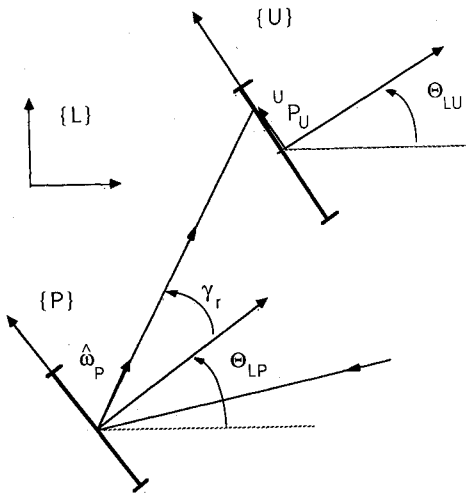

Fig. B3 Example for coordinate determination.

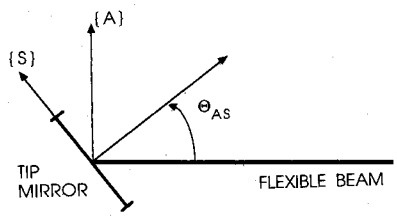

Fig. B4 Auxiliary coordinate frame.

where L is the length of the undeformed beam and ψ_4 is the hub slewing angle.

The following example will illustrate the procedure as we determine the coordinate of the point where the ray hits the hub mirror. Consider mirrors 1 and 2 shown in Fig. B3 with reference frames $\{P\}$ and $\{U\}$, where $\hat{\omega}_p$ is a unit vector in the direction of the reflected ray. Let ${}^U\bar{P}_U = [0\, f]^T$ denote the point where the ray hits mirror 2. The reflected ray can be described as a two-dimensional line given by the set of points

$$z_r = \{z : z = z_o + \rho\hat{\omega}_p\}$$

in $\{P\}$, where z_o denotes the coordinate of the origin of the ray and ρ is a real constant. The intersection of the ray with the hub mirror can be found by solving the expression

$$\begin{bmatrix} {}^UP_U \\ 1 \end{bmatrix} = {}^U_P T \begin{bmatrix} z_o + \rho\hat{\omega}_p \\ 1 \end{bmatrix}$$

from which

$$\rho = \frac{\bar{y}_2 \sin\theta_{LU} + (\bar{x}_2 - \bar{x}_1)\cos\theta_{LU}}{\cos(\theta_{PU} - \gamma_r)}$$

$$-f = \frac{(\bar{x}_1 - \bar{x}_2)\sin(\theta_{LP} + \gamma_r) + \bar{y}_2\cos(\theta_{LP} + \gamma_r)}{\cos(\theta_{LU} - \theta_{LP} - \gamma_r)}$$

where we have used the fact that $\theta_{PU} = \theta_{LU} - \theta_{LP}$, $z_0 = [0\ 0]^T$, and, where, γ_r is the angle of reflection of the ray.

In terms of the fixed reference frame $\{L\}$,

$$\begin{bmatrix} {}^LP_U \\ 1 \end{bmatrix} = {}^L_U T \begin{bmatrix} {}^UP_U \\ 1 \end{bmatrix} \Rightarrow \begin{bmatrix} x_2 \\ y_2 \end{bmatrix} = \begin{bmatrix} \bar{x}_2 + f\sin\theta_{UL} \\ \bar{y}_2 + f\cos\theta_{UL} \end{bmatrix}$$

The remaining coordinates (x_3, y_3), $(x_{\text{hit}}, y_{\text{hit}})$ are obtained in a similar straightforward manner, and we will simply present the final results. Define $\theta_{LP} = \psi_1$, $\theta_{LU} = \psi_2$, and $\theta_{AS} = \psi_3$, as illustrated in Fig. B4. The ray hit coordinates can be shown to be given by

$$x_1 = \bar{x}_1, \qquad y_1 = 0 \tag{B1}$$

$$x_2 = \frac{\bar{y}_2 + \bar{x}_1\tan(2\psi_1) + \bar{x}_2\cot(\psi_2)}{\tan(2\psi_1) + \cot(\psi_2)} \tag{B2}$$

$$y_2 = (x_2 - \bar{x}_1)\tan(2\psi_1) \tag{B3}$$

$$x_3 = \frac{y_2 - \bar{y}_3 + x_2\tan[2(\psi_1 - \psi_2)] - \bar{x}_3\cot(\psi_3 - \psi_4)}{\tan[2(\psi_1 - \psi_2)] - \cot(\psi_3 - \psi_4)} \tag{B4}$$

$$y_3 = y_2 + (x_2 - x_3)\tan[2(\psi_1 - \psi_2)] \tag{B5}$$

$$x_{\text{hit}} = x_S \tag{B6}$$

$$y_{\text{hit}} = y_3 + (x_s - x_3)\tan[2(\psi_1 - \psi_2 + \psi_3 - \psi_4)] \tag{B7}$$

where we have assumed (without loss of generality) that the ray is adjusted to hit the center of mirror 1. Also, to ensure that the ray hits the surfaces of the hub and tip mirrors, the following bounds are imposed on angles ψ_1, ψ_2, ψ_3, and ψ_4:

$$\frac{\bar{y}_2 - \frac{1}{2}\hat{l}\cos(\psi_2)}{\bar{x}_2 + \frac{1}{2}\hat{l}\sin(\psi_2) - \bar{x}_1} < \tan(2\psi_1) < \frac{\bar{y}_2 + \frac{1}{2}\hat{l}\cos(\psi_2)}{\bar{x}_2 - \frac{1}{2}\hat{l}\sin(\psi_2) - \bar{x}_1}$$

$$\frac{\bar{y}_3 - \frac{1}{2}\hat{l}\cos(\psi_3 - \psi_4) - y_2}{x_2 - \frac{1}{2}\hat{l}\sin(\psi_3 - \psi_4) - \bar{x}_3} < \tan[2(\psi_1 - \psi_2)]$$

$$< \frac{\bar{y}_3 + \frac{1}{2}\hat{l}\cos(\psi_3 - \psi_4) - y_2}{x_2 + \frac{1}{2}\hat{l}\sin(\psi_3 - \psi_4) - \bar{x}_3}$$

where $\hat{l}$ is the side length of the mirrors (assumed to be square-shaped).

References

[1]Hughes, R. O., "Conceptual Design of Pointing Control Systems for Space Station Gimballed Payloads," in *Proceedings of the AIAA Guidance, Navigation, and Control Conference*, AIAA, New York, 1986.

[2]Yuan, J. S. and Stieber, M. E., "Robust Beam Pointing and Attitude Control of a Flexible Spacecraft," *Journal of Guidance, Control, and Dynamics*, Vol. 9, March 1986, pp. 228–234.

[3]O'Dell, C. R., "Optical Space Astronomy and Goals of the Large Space Telescope," *Astronautics & Aeronautics*, Vol. 11, Jan. 1973, pp. 22–27.

[4]Hardy, J. W., "Active Optics: A New Technology for the Control of Light," *Proceedings of the IEEE*, Vol. 66, June 1978, pp. 651–697.

[5]Jones, C. O., "Space Telescope Optics," *Optical Engineering*, Vol. 18, May 1979, pp. 273–280.

[6]Chiarappa, D. J. and Claysmith, C. R., "Deformable Mirror Surface Control Techniques," *Journal of Guidance and Control*, Vol. 4, Jan. 1981, pp. 27–34.

[7]Dougherty, H., "Space Telescope Pointing Control System," *Journal of Guidance and Control*, Vol. 5, July 1982, pp. 403–409.

[8]Sandford, T., "Flight Dynamics Laboratory Overview," in *Proceedings of the First NASA/DOD CSI Technology Conference*, Nov. 1986, pp. 41–67.

[9]Founds, D., "Joint Optics Structures Experiment (JOSE)," in *Proceedings of the First NASA/DOD CSI Technology Conference*, Nov. 1986, pp. 591–602.

[10]Pimentel, K. D., "Research Needs in DEW Control Technology," in *Proceedings of the SDIO/LLNL Workshop on Control Systems for DEW*, Livermore, CA, March 1986.

[11]Rew, D. W., and Junkins, J. L., "Some Recent Results on Robustness Optimization for Control of Flexible Structures," in *Proceedings of the VPI & AIAA Symposium on Dynamics and Control of Large Structures*, AIAA, New York, June 1987.

[12]Das, A., Slimak, L. K. S., and Schlaegel, W. T., "Spacecraft Dynamics and Control Programs at AFRPL," in *Proceedings of the First NASA/DOD CSI Technology Conference*, Nov. 1986, pp. 25–40.

[13]Singh, G., Kabamba, P. T., and McClamroch, N. H., "Planar Time Optimal, Rest to Rest, Slewing Maneuvers of Flexible Spacecraft," *Journal of Guidance, Control, and Dynamics* (to be published).

[14]Barbieri, E. and Özgüner, Ü., "Rest-to-Rest Slewing of Flexible Structures in Minimum Time," *Proceedings of the 27th IEEE Conference on Decision and Control*, Inst. of Electrical and Electronics Engineers, New York, 1988, pp. 1633–1638.

[15]Brady, L., Franco, G., Keranen, L., Kern, J., Neiswander, R., and Tung, F., "Vibration Control of Space Structures VCOSS B: Momentum Exchange and Truss Damping," Air Force Wright Aeronautical Lab., Wright-Patterson AFB, OH, AFWAL-TR-83-3075, 1983.

[16]Aubrun, J. N., Lorell, K. R., Havas, T. W., and Henninger, W. C., "An Analysis of the Segment Alignment Control System for the W. M. Keck Observatory Ten Meter Telescope," Keck Observatory, TR-143 (Final Rept.) 1985.

[17]Özgüner, Ü., Yurkovich, S., Martin, J., and Al-Abbass, F., "Decentralized Control Experiments on NASA's Flexible Grid," in *Proceedings of the 1986 American Control Conference*, Seattle, WA, June 1986, pp. 1045–1051.

[18]Yurkovich, S., Özgüner, Ü., and Al-Abbass, F., "Model Reference, Sliding Mode Adaptive Control for Flexible Structures," *Journal of the Astronautical Sciences* (to be published).

[19]Schaechter, D., "Optimal Local Control of Flexible Structures," *Journal of Guidance and Control*, Vol. 4, Jan. 1981, pp. 22–26.

[20]Hughes, P. C., "Dynamics of Flexible Space Vehicles with Active Attitude Control," *Celestial Mechanics*, Vol. 9, 1974, pp. 21–39.

[21]Hablani, H. B., "Constrained and Unconstrained Modes: Some Modeling Aspects of Flexible Spacecraft," *Journal of Guidance and Control*, Vol. 5, March–April 1982, pp. 164–173.

[22]Barbieri, E. and Özgüner, Ü., "Unconstrained and Constrained Mode Expansions for a Flexible Slewing Link," *ASME Transactions Journal of Dynamic Systems, Measurement, and Control* (to be published); also, *Proceedings of American Control Conference*, Atlanta, GA, June 1988.

[23]Barbieri, E., "An Integrated Structural-Control Model of the OSU Pichon System," Control Research Lab., Ohio State Univ., Columbus, OH, TR CRL-1026-Su87-R, Aug. 1987.

[24]İftar, A. and Özgüner, Ü., "A Linear-Quadratic Optimal Solution to the Decentralized Servomechanism Problem with Robust Noisy Controllers," in *Proceedings of the IEEE Conference on Decision and Control*, Institute of Electrical and Electronic Engineers, New York, Dec. 1987, pp. 2314–2319.

[25]Barbieri, E., Yurkovich, S., and Özgüner, Ü., "Control of Multiple-Mirror/Flexible-Structures in Slew Maneuvers," in *Proceedings of the AIAA Guidance, Navigation, and Control Conference*, AIAA, New York, pp. 379–388.

[26]Özgüner, Ü., "Decentralized/Relegated Control," in *Proceedings of the ICES-88*, Atlanta, GA, April 1988 (to be published).

[27]Özgüner, Ü. and Yurkovich, S., "New Directions in Decentralized/Relegated Control of Large Space Structures," Control Research Lab., Ohio State Univ., Columbus, OH, TR CRL-1005-Su86-R, June 1986.